Enhanced fatty acid oxidation in adipocytes and macrophages reduces lipid-induced triglyceride accumulation and inflammation

Maria Ida Malandrino[1,2], Raquel Fucho[1,2], Minéia Weber[1,2], María Calderon-Dominguez[1,2], Joan Francesc Mir[1,2], Lorea Valcarcel[1,2], Xavier Escoté[3,4], María Gómez-Serrano[2,5], Belén Peral[2,5], Laia Salvadó[4,6], Sonia Fernández-Veledo[3,4], Núria Casals[2,7], Manuel Vázquez-Carrera[4,6], Francesc Villarroya[1,2], Joan J Vendrell[3,4], Dolors Serra[1,2], Laura Herrero[1,2]

[1]Department of Biochemistry and Molecular Biology, Institut de Biomedicina de la Universitat de Barcelona (IBUB), Universitat de Barcelona, E-08028 Barcelona, Spain

[2]CIBER Fisiopatología de la Obesidad y la Nutrición (CIBEROBN), Instituto de Salud Carlos III, Madrid, Spain

[3]Endocrinology and Diabetes Unit. Joan XXIII University Hospital, IISPV, Universitat Rovira i Virgili, E-43007 Tarragona, Spain.

[4]CIBER de Diabetes y Enfermedades Metabólicas Asociadas (CIBERDEM), Instituto de Salud Carlos III, Madrid, Spain

[5]Instituto de Investigaciones Biomédicas Alberto Sols, Consejo Superior de Investigaciones Científicas and Universidad Autónoma de Madrid (CSIC-UAM), E-28029 Madrid, Spain

[6]Pharmacology Unit, Department of Pharmacology and Therapeutic Chemistry and IBUB, Faculty of Pharmacy, University of Barcelona, Barcelona, Spain

[7]Basic Sciences Department, Faculty of Medicine and Health Sciences, Universitat Internacional de Catalunya, E-08195 Sant Cugat del Vallés, Barcelona, Spain

Address correspondence to:
Laura Herrero, PhD
Department of Biochemistry and Molecular Biology, IBUB
School of Pharmacy
University of Barcelona
Av. Diagonal, 643
E-08028 Barcelona, Spain
Tel: (+34) 934 024 522
Fax: (+34) 934 024 520
Email: lherrero@ub.edu

Running head

Fatty acid oxidation in adipocytes and macrophages

Conflict of interest statement

All authors declare no conflict of interest to disclose.

ABSTRACT

Lipid overload in obesity and type 2 diabetes is associated with adipocyte dysfunction, inflammation, macrophage infiltration and decreased fatty acid oxidation (FAO). Here we report that the expression of carnitine palmitoyltransferase 1A (CPT1A), the rate-limiting enzyme in mitochondrial FAO, is higher in human adipose tissue macrophages than in adipocytes and that it is differentially expressed in visceral *vs.* subcutaneous adipose tissue both in an obese and a type 2 diabetes cohort. These observations led us to further investigate the potential role of CPT1A in adipocytes and macrophages. We expressed CPT1AM, a permanently active mutant form of CPT1A, in 3T3-L1 CARΔ1 adipocytes and RAW 264.7 macrophages through adenoviral infection. Enhanced FAO in palmitate-incubated adipocytes and macrophages reduced triglyceride content and inflammation, improved insulin sensitivity in adipocytes and reduced ER stress and ROS damage in macrophages. We conclude that increasing FAO in adipocytes and macrophages improves palmitate-induced derangements. This indicates that enhancing FAO in metabolically relevant cells such as adipocytes and macrophages may be a promising strategy for the treatment of chronic inflammatory pathologies such as obesity and type 2 diabetes.

Keywords

Obesity, type 2 diabetes, adipocytes, macrophages, inflammation, fatty acid oxidation, CPT1.

Abbreviations

Ad, adenovirus; AGPAT5, 1-acylglycerol-3-phosphate O-acyltransferase 5; BCL2, B-cell CLL/lymphoma 2; CD163, macrophage and monocyte marker; CHOP, C/EBP homologous protein; CPT1A, carnitine palmitoyltransferase 1A; CPT1AM, carnitine palmitoyltransferase 1A (permanently active mutant form); EDEM, ER degradation enhancing α-mannosidase-like protein; ER, endoplasmic reticulum; FA, fatty acids; FAO, fatty acid oxidation; GFP, green fluorescent protein; IL-1β, interleukin-1β; IL-6, interleukin-6; IRbeta, insulin receptor beta; MCP-1, monocyte chemoattractant protein-1; moi, multiplicity of infection; PDI, protein disulfide isomerase; ROS, reactive oxygen species; SAT, subcutaneous adipose tissue; SREBF1, Sterol regulatory element binding transcription factor 1; SVF, stromal-vascular fraction; TLR-4, toll-like receptor-4; VAT, visceral adipose tissue; WAT, white adipose tissue.

INTRODUCTION

Obesity has reached epidemic proportions worldwide, leading to severe associated pathologies such as insulin resistance, type 2 diabetes (T2D), cardiovascular disease, Alzheimer's disease, hypertension, hypercholesterolemia, hypertriglyceridemia, non-alcoholic fatty liver disease (NAFLD), arthritis, asthma, and certain forms of cancer (12).

Over the last two decades adipose tissue has gained crucial importance in the mechanisms involved in obesity-related disorders. The energy-storing white adipose tissue (WAT) is well vascularized and contains adipocytes, connective tissue and numerous immune cells such as macrophages, T and B cells, mast cells and neutrophils that infiltrate and increase their presence during obesity (22). Macrophages were the first immune cells reported to participate in obesity-induced insulin resistance (56). This highlights their pathological role in adipose tissue in addition to their traditional involvement in tissue repair and in response to dead and dying adipocytes (5, 14). Fat is an active endocrine tissue that secretes hormones such as leptin, adiponectin or resistin and inflammatory cytokines such as TNF-α, IL-6, IL-1β, etc. in response to several stimuli. It is therefore a complex organ controlling energy expenditure, appetite, insulin sensitivity, endocrine and reproductive functions, inflammation and immunity (53).

The pathophysiology of obesity-induced insulin resistance has been attributed to ectopic fat deposition (39), increased inflammation and ER stress (16, 42), adipose tissue hypoxia (15) and mitochondrial dysfunction (32), and impaired adipocyte expansion and angiogenesis (50, 51, 54). In obesity, fatty acids (FA) together with other stimuli such as ceramide, various PKC isoforms, proinflammatory cytokines and ROS and ER stresses activate JNK, NF-κB, RAGE and TLR pathways both in adipocytes and macrophages triggering inflammation and insulin resistance (43).

Strenuous efforts are being made by the research community to elucidate the mechanisms involved in the pathophysiology of obesity-related disorders. However, an alternative strategy could be to act upstream by preventing the accumulation of lipids and the progression of obesity. In addition to reducing caloric intake, a potential effective approach to combat obesity would be to increase energy expenditure in key metabolic organs, such as adipose tissue. Obese individuals and those with T2D are known to have lower fatty acid oxidation (FAO) rates and lower electron transport chain activity in muscle (17, 19, 37) together with higher glycolytic capacities and enhanced cellular FA uptake compared to non-obese and non-diabetic individuals (44). Thus, any strategy able to eliminate the excess of lipids found in obesity could be beneficial for health. Lipid levels can be reduced by inhibiting synthesis, transport or by increasing oxidation: here we focus on the latter.

Malonyl-CoA, derived from glucose metabolism and the first intermediate in lipogenesis, regulates FAO by inhibiting carnitine palmitoyltransferase 1 (CPT1). This makes CPT1 the rate-limiting step in mitochondrial FA β-oxidation. Thus, in high-energy conditions malonyl-CoA inhibits oxidation diverting FAs fate into TG accumulation. There are three CPT1 isoforms, with differential tissue expression: CPT1A (liver, kidney, intestine, pancreas, ovary and mouse and human WAT), CPT1B (brown adipose tissue, skeletal muscle, heart and rat and human WAT), and CPT1C (brain and testis) (2, 36). The fact that CPT1 controls FAO makes it a very attractive target to reduce lipid levels and fight against obesity and T2D. In spite of their excess fat, obese individuals have reduced visceral WAT CPT1 mRNA and protein levels (20). This prompted our group and others to overexpress CPT1 in liver (26, 30, 46), muscle (4, 33, 41), and white adipocytes (9), which led to a decrease in TG content and an improvement in insulin sensitivity.

Here we showed that CPT1A expression was higher in human adipose tissue macrophages than in mature adipocytes and that it was differentially expressed in visceral *vs.* subcutaneous adipose tissue. To further investigate the role of CPT1A in both adipocytes and macrophages we used a permanently active mutant form of CPT1A, CPT1AM, which is insensitive to its inhibitor malonyl-CoA (27), to achieve continuous oxidation of lipids. When cells were incubated with palmitate to mimic obesity, CPT1AM restored most of the palmitate-induced imbalances. An increase in FAO in adipocytes and macrophages reduced TG content and inflammatory levels, improved insulin sensitivity in adipocytes, and reduced endoplasmic reticulum (ER) stress and ROS damage in macrophages.

MATERIALS AND METHODS

Human cohorts

Selection of patients

Adipose tissue was selected from an adipose tissue biobank collection of the University Hospital Joan XXII (Tarragona, Spain). All subjects were of Caucasian origin and reported that their body weight had been stable for at least 3 months before the study. They had no systemic disease other than obesity or T2D, and all had been free of any infections in the previous month before the study. Liver and renal diseases were specifically excluded by biochemical work-up. Appropriate Institutional Review Board approval and adequate biobank informed consent was obtained from all participants. Bio-banking samples included plasma, total and fractionated adipose tissue from subcutaneous and visceral origin. All patients had fasted overnight before collection of blood and adipose tissue samples. Visceral adipose tissue (VAT) and subcutaneous adipose tissue (SAT) samples were obtained during surgical procedures that included laparoscopic surgery for hiatus hernia repair or cholecystectomy. Samples were selected according stratification by age, gender and BMI and grouped into two cohorts:

Obesity cohort. Subjects were classified by BMI according to the World Health Organization criteria (WHO, 2000). The study included 19 lean, 28 overweight, and 15 obese non-diabetic subjects, matched for age and gender (Table 1).

Type 2 diabetes cohort. Patients were classified as having T2D according to the American Diabetes Association criteria (1997). Variability in metabolic control was assessed by stable glycated hemoglobin A1c (HbA1c) values during the previous 6 months. Gathering these criteria, there were 11 T2D subjects. As a control group, we selected 36 subjects without diabetes from the obesity cohort, matched for age, BMI and gender (Table 2). No patient was being treated with thiazolidinedione.

168

169 *Anthropometric measurements*

170 Height was measured to the nearest 0.5 cm and body weight to the nearest 0.1 kg. BMI
171 was calculated as weight (kilograms) divided by height (meters) squared. Waist
172 circumference was measured midway between the lowest rib margin and the iliac crest.

173

174 *Collection and processing of human samples*

175 Samples from VAT (visceral adipose tissue, omental) and SAT (subcutaneous adipose
176 tissue, anterior abdominal wall) from the same individual were obtained during
177 abdominal elective surgical procedures (cholecystectomy or surgery for abdominal
178 hernia). All patients had fasted overnight, at least 12 hours before surgical procedure.
179 Blood samples were collected before the surgical procedure from the antecubital vein,
180 20 ml of blood with EDTA (1mg/ml) and 10 ml of blood in silicone tubes. 15 ml of
181 collected blood was used for the separation of plasma. Plasma samples were stored at -
182 80ºC until analytical measurements were performed. 5 ml of blood with EDTA was
183 used for the determination of HbA1c. Adipose tissue samples were collected, washed in
184 PBS, immediately frozen in liquid N_2 and stored at -80°C.

185

186 *Adipose tissue fractionation*

187 Adipose tissue biopsies were immediately processed. The adipose tissue was finely
188 diced into small pieces (10-30 mg), washed in PBS and incubated in Medium 199 (Life
189 Technologies) supplemented with 4% BSA plus 2 mg/ml of collagenase Type I (Sigma)
190 for 1 h in a shaking water bath at 37ºC. After digestion, mature adipocytes (ADI) were
191 separated from tissue matrix by filtration through a 200 µm mesh fabric (Spectrum
192 Laboratories). The filtrated solution was centrifuged for 5 min at 1500x*g*. The mature

adipocytes were removed from the top layer and the SVF cells remained in the pellet. Cells were washed 4 times in PBS and processed for RNA and protein extraction.

Analytical methods

Glucose, cholesterol and TG plasma levels were determined in an auto-analyser (Hitachi 737, Boehringer Mannheim) using the standard enzyme methods. High-density lipoprotein (HDL) cholesterol was quantified after precipitation with polyethylene glycol at room temperature (PEG-6000). Plasma insulin was determined by radioimmunoassay (Coat-A-Count insulin; Diagnostic Products Corp.). Non-esterified Free Fat Acid (NEFA) serum levels were determined in an autoanalyser (Advia 1200, Siemens AG) using an enzymatic method developed by Wako Chemicals. Plasma glycerol levels were analyzed by using a free glycerol determination kit, a quantitative enzymatic determination assay (Sigma-Aldrich Corp.). Intra- and interassay CV were less than 6% and less than 9.1%, respectively. The degree of insulin resistance was determined by the homeostasis model assessment (HOMA), as [glucose (mmol/l) x insulin (mIU/l)]/22.5](24).

Immunohistochemistry

Five-micron sections of formalin-fixed paraffin-embedded adipose tissue were deparaffinised and rehydrated prior to antigen unmasking by boiling in 1mM EDTA, pH 8. Sections were blocked in normal serum and incubated overnight with rabbit anti-CPT1A (Sigma-Aldrich) at 1:50 dilution. Secondary antibody staining was performed using the VECTASTAIN ABC kit (Vector Laboratories, Inc.) and detected with diaminobenzidine (DAB, Vector Laboratories, Inc.). Sections were counterstained with hematoxylin prior to dehydration and coverslip placement, and examined under a Nikon

Eclipse 90i microscope. As a negative control, the procedure was performed in the absence of primary antibody.

Immunofluorescence

Five-micron sections of formalin-fixed paraffin-embedded adipose tissue were blocked in normal serum and incubated overnight with rabbit anti-CPT1A antibody (Sigma-Aldrich) at 1:50 dilution, and with mouse anti-CD68 (Santa Cruz Biotechnology, Inc.) at 1:50 dilution, washed, and visualized using Alexa Fluor 546 goat anti-rabbit, and Alexa Fluor 488 goat anti-mouse antibodies, respectively (1:500; Molecular Probes Inc.). The slides were counterstained with DAPI (4,6-diamidino-2-phenylindole) to reveal nuclei and were examined under a Nikon Eclipse 90i fluorescent microscope. As a negative control, the assay was performed in the absence of primary antibody.

Materials

Sodium palmitate, sodium oleate, BSA and L-carnitine hydrochloride were purchased from Sigma Aldrich. DMEM, FBS and Penicillin/Streptomycin mixture were purchased from Life Technologies.

Cell culture

Murine 3T3-L1 CARΔ1 preadipocytes, kindly given by Dr. Orlicky (Department of Pathology, UCHSC at Fitzsimons, Aurora, CO, USA), were cultured and differentiated into mature adipocytes following the published protocol (31). Mature adipocytes were used for experiments at day 8 post-differentiation. Murine RAW 264.7 macrophages were obtained from ATCC and were maintained in DMEM supplemented with 10% heat-inactivated FBS and 1% penicillin/streptomycin mixture. Simpson-Golabi-Behmel

Syndrome (SGBS) human cells were cultured and differentiated to adipocytes as previously described (55).

Adenovirus (Ad) infection

At day 8 of differentiation, 3T3-L1 CARΔ1 cells were infected with AdGFP (100 moi) and AdCPT1AM (13) (100 moi) for 24 h in serum-free DMEM and then the medium was replaced with complete DMEM for additional 24 h. RAW 264.7 macrophages were infected with AdGFP (100 moi) and AdCPT1AM (100 moi) for 2 h in serum-free DMEM and then replaced with complete medium for additional 72 h. The adenovirus infection efficiency was assessed in AdGFP-infected cells (Figure 3A and B). The same batch of adenoviruses stored in 50µl aliquots was used throughout the experiments.

Fatty acid (FA) treatment

Sodium palmitate was conjugated with FA-free BSA in a 5:1 ratio to yield a stock solution of 2.5mM (41). Cells were incubated with 0.3 mM or 1 mM of this solution for 24 h (3T3-L1 CARΔ1 adipocytes) or 0.3 mM, 0.5 mM or 0.75 mM for 24, 8 or 18 h (RAW 264.7 macrophages), respectively.

Adipocyte and macrophage viability

3T3-L1 CARΔ1 adipocytes and RAW 264.7 macrophages were infected as previously described and incubated for 24h with 1mM or 0.3mM palmitate, respectively. Cells were washed twice with PBS and lifted from the surface with trypsin followed by 2 min incubation at 37ºC. Trypsinization was stopped with 10% FBS containing media and equal volumes of cell suspension were mixed with 0.4% Trypan blue staining. Trypan blue positive and negative cells were counted using a Neubauer chamber for adipocytes

and Countess Automated Cell Counter (Invitrogen) for macrophages. Percentage of viability was determined normalizing viable cells of each group to viable cells of BSA GFP group. Statistical significance was assessed using two-way Anova analysis of three individual experiments (* $p<0.05$).

CPT1 activity

Mitochondria-enriched fractions were obtained from cell culture grown in 10-cm^2 dishes and CPT1 activity was measured by a radiometric method as described (13).

Fatty acid oxidation

Total oleate oxidation was measured in 3T3-L1 CARΔ1 adipocytes and RAW 264.7 macrophages grown in 25-cm^2 flasks, differentiated, and infected as described above. The day of the assay cells were washed in KRBH 0.1% BSA, preincubated at 37°C for 30 min in KRBH 1% BSA, and washed again in KRBH 0.1% BSA. Cells were then incubated for 3 h (3T3-L1 CARΔ1 adipocytes) or 2 h (RAW 264.7 macrophages) at 37°C with fresh KRBH containing 11 mM glucose, 0.8 mM carnitine plus 0.2 mM [1-^{14}C] oleate (Perkin Elmer). Oxidation was measured as described (30). The scintillation values were normalized to the protein content of each flask.

TG content

Cells were grown in 12-well plates, differentiated and infected as described above. After 24 h (3T3-L1 CARΔ1 adipocytes) or 18 h (RAW 264.7 macrophages) of FA treatment, cells were collected for lipid extraction following Gesta *et al* protocol (10) with minor modifications: after cell lysis with 0.1% SDS, 1/2/0.12 (v/v/v) methanol/chloroform/0.5M KCl solution was added, the two phases were separated by

293 centrifugation and the upper phase was dried with N_2. Finally, lipids were resuspended
294 in 100% isopropanol and TG were quantified using TG Triglyceride kit (Sigma),
295 according to the manufacturer's instructions. Protein concentrations were used to
296 normalize sample values.
297
298 *Oil Red O staining*
299 RAW 264.7 macrophages grown on coverslips were infected as described above and
300 incubated with 0.75 mM of palmitate for 18 hours. After this time, cells were rinsed
301 twice with PBS, fixed in 10% paraformaldehyde for 30 minutes at room temperature
302 and washed again with PBS. Then, cells were rinsed with 60% isopropanol for 5 min to
303 facilitate the staining of neutral lipids and stained with filtered Oil Red O working
304 solution (0.3 % Oil Red O in isopropanol) for 15 min. After several washes with
305 distilled water the coverslips were removed and mounted on a drop of mount medium.
306 The intracellular lipid vesicles stained with Oil Red O were identified by their bright red
307 color under the microscope.
308
309 *Analysis of intracellular protein oxidation*
310 RAW 264.7 macrophages were cultured in 12-well plates and infected as described
311 before. After FA treatment, cell extracts were prepared and analyzed for protein
312 oxidative modifications (*i.e.* carbonyl group content) with OxyBlot Protein Oxidation
313 Detection kit (Millipore), following the manufacturer's instructions.
314
315 *Western blot analysis*
316 3T3-L1 CARΔ1 adipocytes and RAW 264.7 macrophages were cultured in 12-well
317 plates, differentiated, and infected as described above. Cells were collected in lysis

buffer (RIPA) and protein concentration was determined using the BCA protein assay kit (Thermoscientific). Equal amount of protein from whole cell lysates was resolved by 8% SDS-PAGE and transferred to PVDF membranes (Millipore). Signal detection was carried out with the ECL immunoblotting detection system (GE Healthcare) and the results were quantitatively analyzed using Image Quant LAS4000 Mini (GE Healthcare). The following antibodies were used: CPT1A (1/6,000; (13)), β-actin (I-19) (1/4,000;Santa Cruz), Akt and pAkt (Ser^{473}) (1/1,000; Cell Signaling), CHOP (GADD 153; 1/200; Santa Cruz) and IRbeta (1/1,000; Santa Cruz). Human fat tissue was homogenized in RIPA buffer as previously described (34). Protein extracts (10-20 μg) were loaded, resolved on 10% SDS-PAGE and transferred to Hybond ECL nitrocellulose membranes. Membranes were stained with 0.15% Ponceau red (Sigma-Aldrich) to ensure equal loading after transfer and then blocked with 5% (w/v) BSA in TBS buffer with 0.1% Tween 20. Immunoblotting was performed with 1:2000 goat anti-human CPT1A (Abcam). Blots were incubated with the appropriate IgG-HRP-conjugated secondary antibody. Immunoreactive bands were visualized with an ECL-plus reagent kit (GE Healthcare). Optical densities of the immunoreactive bands were measured using Image J analysis software.

Analysis of mRNA expression by quantitative real-time PCR

Total RNA was extracted from cultured cells grown in 12-well plates using Illustra MiniRNA Spin kit (GE Healthcare) and cDNA was obtained using Transcriptor First Strand cDNA Synthesis kit (Roche). Quantitative real-time PCR was performed using SYBR Green PCR Master Mix Reagent Kit (Life Technologies). Levels of mRNA were normalized to those of β-actin and expressed as fold change. Forward/reverse primers for several used genes (other sequences are available upon request):

343

	FORWARD	REVERSE
β-ACTIN	5'- AGGTGACAGCATTGCTTCTG- 3'	5'- GCTGCCTCAACACCTCAAC-3'
CHOP	5´-CCCTGCCTTTCACCTTGG- 3'	5´-CCGCTCGTTCTCCTGCTC- 3'
CPT1A*	5'- GCAGCAGATGCAGCAGATCC- 3'	5'-TCAGGATCCTCCTCTCTGTATCCC3'
EDEM	5'-AAGCCCTCTGGAACTTGCG- 3'	5'-AACCCAATGGCCTGTCTGG- 3'
GRP78	5´-ACTTGGGGACCACCTATTCCT- 3'	5´-ATCGCCAATCAGACGCTCC- 3'
IL-1β	5'- GCCCATCCTCTGTGACTCAT- 3'	5'- AGGCCACAGGTATTTTGTCG- 3'
MCP-1	5'- TCCCAATGAGTAGGCTGGAG-3'	5'- AAGTGCTTGAGGTGGTTGTG- 3'
PDI	5'-ACCTGCTGGTGGAGTTCTATG- 3'	5'-CGGCAGCTTTGGCATACT- 3'
TLR-4	5'- GGACTCTGATCATGGCACTG- 3'	5'- CTGATCCATGCATTGGTAGGT- 3'
TNF-α	5'-ACGGCATGGATCTCAAAAGAC-3'	5'-AGATAGCAAATCGGCTGAACG- 3'

344 * Recognizes both CPT1A and CPT1AM

345 400-500mg frozen human adipose tissue was homogenized with an Ultra-Turrax
346 8 (Ika). Total RNA from adipose biopsies, stromal-vascular fractions (SVF) and isolated
347 adipocytes were extracted by using RNeasy Lipid Tissue Midi Kit (QIAGEN Science)
348 following the manufacturer's instructions and total RNA was treated with 55 U RNase-
349 free DNase (QIAGEN) to avoid contamination with genomic DNA. Between 0.2 and 1
350 μg of total RNA was reverse-transcribed to cDNA using TaqMan Reverse Transcription
351 reagents (Applied Biosystems), and subsequently diluted with nuclease-free water
352 (Sigma) to 20 ng/μl cDNA. For adipose tissue gene expression analysis a real-time
353 quantitative PCR was performed, with duplicates, on a 7900HT Fast Real-Time PCR
354 System using commercial Taqman Assays (Applied Biosystems). SDS software 2.3 and
355 RQ Manager 1.2 (Applied Biosystems) were used to analyse the results with the
356 comparative threshold cycle (Ct) method ($2^{\Delta\Delta Ct}$). C_t values for each sample were
357 normalized with an optimal reference gene (cyclophilin), after testing three additional

housekeeping genes: β-actin and RNA 18S. A panel of genes involved in the adipocyte differentiation and metabolism was selected in the study of CPT1A gene expression:

GEN SIMBOL	GENE DENOMINATION	ASSAI ID
ACC1	(acetyl-coenzyme carboxylase 1) ACACA	Hs00167385_m1
PCK2	(phosphoenolpyruvate carboxykinase 2)	Hs00388934_m1
PPARα	(peroxisome proliferator-activated receptor α)	Hs00231882_m1
PPARγ	(peroxisome proliferator-activated receptor λ)	Hs00234592_m1
AGPAT3	(1-acyl-sn-glycerol-3-phosphate acyltransferase gamma / LPAAT-g1)	Hs00987571_m1
AGPAT4	(1-acyl-sn-glycerol-3-phosphate acyltransferase / LPAAT-d)	Hs00220031_m1
AGPAT5	(1-acyl-sn-glycerol-3-phosphate acyltransferase / LPAAT-e)	Hs00218010_m1
AGPAT9	(1-acylglycerol-3-phosphate O-acyltransferase 9/ LPAAT-theta)	Hs00262010_m1
CDS1	(phosphatidate cytidylyltransferase)	Hs00181633_m1
PCYT1A	(choline-phosphate cytidylyltransferase)	Hs00192339_m1
PCYT2	(ethanolamine-phosphate cytidylyltransferase	Hs00161098_m1
PDE3B	(phosphodiesterase type 3)	Hs01057215_m1
FDFT1	(farnesyl-diphosphate farnesyltransferase 1)	Hs00926054_m1
SREBF1	(sterol regulatory element binding transcription factor 1)	Hs01088691_m1
BCL2	(B-cell CLL/lymphoma 2)	Hs99999018_m1
CD163	Macrophage and monocyte marker	Hs01016661 _m1
CPT1A	(carnitine palmitoyltransferase 1A)	Hs00912676_m1

Cytokines measurement in culture media

Cytokines protein levels in culture media of 3T3-L1 CARΔ1 adipocytes and RAW 264.7 macrophages were measured by Luminex technology with a MILLIPLEX Analyzer Luminex 200x Ponenet System (MCYTOMAG-70K-08 Mouse Cytokine MAGNETIC Kit; Merck Millipore).

Analysis of cellular redox status

To detect ROS (superoxide) formation, MitoSOX Red (M36008 - Life Techonologies) fluorescence was measured by flow cytometry. RAW 264 cells were infected with 100 moi AdCPT1AM (or AdGFP as control) for 48h; then 16h prior to ROS measurement, macrophages were treated with 0.75 mM palmitate BSA-conjugated (or with BSA as control). Medium was removed and cells were incubated for 30 min with PBS containing 5 μM MitoSOX Red. The labeled macrophages were washed three times with HBSS/Ca/Mg, pelleted, resuspended in 300 μl HBSS/Ca/Mg and fixed by adding 1.2 ml absolute ethanol and keeping them at -20ºC for 5 minutes. Cells were pelleted again and resuspended in HBSS/Ca/Mg containing 3 μM DAPI, to mark their nuclei. Then macrophages were analyzed by flow cytometry (Gallios Cytometer - Beckman Coulter). The fluorescence intensity of MitoSOX Red was measured using excitation at 510 nm and emission at 580 nm.

Statistical analysis

Data are expressed as the mean ± SEM and analyzed statistically using Student's *t*-test (column analysis) or two-way ANOVA (grouped analysis). All figures and statistical analyses were generated using GraphPad Prism 6. $P<0.05$ was considered statistically significant. For human data statistical analyses were performed with SPSS 12.0 (SPSS). Results are expressed as mean ± SD. The non-normally distributed variables were represented as the median (interquartile range). Categorical variables were reported by number (percentages). Student's t test analysis was used to compare the mean value of normally distributed continuous variables. Variables with a non-Gaussian distribution were analyzed by using non-parametric test (Kruskal-Wallis, or Mann-Whitney test for

392 independent samples or Wilcoxon test for related samples when necessary).
393 Associations between continuous variables are sought by correlation analyses. Finally a
394 stepwise multiple linear regression analysis is performed to determine independent
395 variables associated with CPT1A gene expression levels in SAT and VAT depot.
396 Results are expressed as unstandardized coefficient (B), and 95% confidence interval
397 for B (95%CI(B)). Differences are considered significant if a computed two-tailed
398 probability value (P) is < 0.05.
399
400

RESULTS

CPT1A expression pattern in human adipose tissue from obese and diabetic patients

Visceral and subcutaneous adipose tissue (VAT and SAT, respectively) were analyzed from both an obesity cohort (lean, overweight and obese patients) and a T2D cohort (control and T2D patients). Tables 1 and 2 show the phenotypic and metabolic characteristics and CPT1A expression levels of the subjects. No differences in CPT1A gene expression levels either in SAT or in VAT depots were observed when comparing with the non-obese or the non-diabetic counterparts (Fig. 1A and B; Tables 1 and 2). However, in the obesity cohort, CPT1A mRNA expression was significantly higher in lean and overweight VAT than in SAT (Fig. 1A). This difference was lost in the obese patients. These results were corroborated by Western blot with human adipose tissue of several lean and obese individuals (Fig. 1C and D, P=0.015). Similar results were obtained in the T2D cohort, where control subjects showed significantly higher CPT1A mRNA levels in VAT *vs.* SAT (Fig. 1B). However, this difference disappeared in T2D patients. Despite T2D patients showed a trend to express higher CPT1A levels in SAT and VAT compared to controls (on the opposite than in the obese subjects) this difference was non-significant. Since CPT1B isoform is also expressed in human adipose tissue we analyzed CPT1B mRNA (Fig. 1E and F) and protein (data not shown) levels in human VAT and SAT of the obesity and the T2D cohort. No differences were seen among the groups.

In order to establish the main relationship between CPT1A gene expression and key adipocyte genes involved in differentiation and metabolic pathways we explored a panel of genes (listed in Material and Methods) both in SAT and VAT depots of the obesity cohort. Results are shown from those genes that changed the most (up or down)

(Tables 3 and 4). Simple association analysis showed an inverse correlation between CPT1A and PPAR-γ in SAT (r= -0.38, P= 0.002) (Table 3). Positive CPT1A correlation both in VAT and SAT was found with AGPAT5 (phospholipid biosynthesis), SREBF1 (glucose and lipid metabolism), BCL2 (anti-apoptosis) and CD163 (macrophage marker) (Table 3).

To study the main determinants of CPT1A gene expression levels, a stepwise multiple regression analysis was performed, including the above-mentioned bivariate associations and confounding factors such as BMI, age and gender. This model showed that SAT CPT1A was positively associated with AGPAT5, SREBF1 and CD163 and that VAT CPT1A was positively correlated with SREBF1 and CD163 and negatively with age and PPAR-γ (Table 4). The inverse relationship between CPT1A and PPAR-γ was corroborated with the human adipocyte cell line SGBS. CPT1A mRNA expression dropped to a new steady state in adipocytes that was 11% of its expression in fibroblasts (data not shown).

CPT1A is highly expressed in human adipose tissue macrophages

To determine the cellular distribution of CPT1A gene and protein in human adipose tissue biopsies, we performed qRT-PCR and immunostaining analysis on both adipose and stromal-vascular fraction (SVF). CPT1A mRNA levels were 42.6-, and 43.4-fold increased in the SVF compared to mature adipocytes in both human SAT ($P<0.05$) and VAT ($P<0.05$), respectively (Fig. 2A). Immunohistological examination of SAT from obese subjects revealed CPT1A+ cells mostly in the SVF (Fig. 2B). Immunofluorescence detection showed a bright staining pattern in cells resembling adipose tissue macrophages. Co-staining analysis using CPT1A and CD68 (a macrophage marker) antibodies confirmed the expression of CPT1A in macrophages

451 (Fig. 2C). Macrophages seem to localize forming the so-called "crown-like structures"
452 surrounding the adipocytes.
453
454 **CPT1AM-expressing adipocytes show enhanced FAO and reduced TG content**
455 To further study the role of CPT1A in adipocytes and macrophages we decided
456 to continue with *in vitro* studies. Since 3T3-L1 adipocytes are inefficiently infected with
457 adenovirus we decided to use the high-infection efficiency white adipocyte cell culture
458 line, 3T3-L1 CARΔ1 adipocytes (31) (Fig. 3A). Cells were transduced for the first time
459 with adenoviruses carrying the CPT1AM gene or GFP as a control. Interestingly,
460 CPT1AM-expressing adipocytes were partially protected from palmitate induced cell
461 death (Fig. 3C).
462 CPT1A mRNA, protein and activity levels were increased in CPT1AM-
463 expressing adipocytes compared to GFP control cells (Fig. 4A-C). CPT1AM-expressing
464 adipocytes retained most of the CPT1 activity after incubation with the CPT1A inhibitor
465 malonyl-CoA (Fig. 4C). FAO rate was concordantly enhanced (1.37-fold increase,
466 $P<0.05$) in CPT1AM-expressing adipocytes (Fig. 4D). FA undergoing β-oxidation yield
467 acetyl-CoA moieties that have two main possible fates: (1) complete oxidation to CO_2
468 and ATP production, or (2) conversion to ketone bodies (mainly in the liver). Here, total
469 FAO rate was calculated as the sum of acid soluble products plus CO_2 oxidation.
470 CPT1AM expression blocked the palmitate-induced increase in TG content (Fig. 4E).
471
472 **Enhanced adipocyte FAO improves insulin sensitivity and reduces inflammation**
473 We examined the effect of increased FAO on insulin sensitivity and
474 inflammatory responses in 3T3-L1 CARΔ1 adipocytes infected with AdCPT1AM.
475 Palmitate-induced decrease in insulin-stimulated Akt phosphorylation and insulin

receptor beta (IRbeta) protein levels was partially restored in CPT1AM-expressing adipocytes (Fig. 4F-H). Palmitate-induced increase of proinflammatory markers (IL-1β, MCP-1 and IL-1α) mRNA and protein levels was blunted in CPT1AM-expressing adipocytes (Fig. 4I-K). Several palmitate concentrations and times of incubation were used to better fit the different dose- and time-response of the cytokines and parameters measured. Consistent with previous studies (9, 11), palmitate incubation raised cytokines expression by 2-3-fold.

Increased FAO in CPT1AM-expressing macrophages protects from palmitate-induced TG accumulation

Since CPT1A was highly expressed in the SVF, and particularly in macrophages, of human adipose tissue we decided to further analyze the effect of an increased FAO on cultured macrophages. RAW 264.7 macrophages were efficiently infected with AdCPT1AM (Fig. 3B). CPT1AM-expressing macrophages were protected from palmitate induced cell death (Fig. 3D). CPT1AM-expressing macrophages showed a 2.4-fold ($P<0.01$) increase in CPT1A mRNA levels, 6.6-fold ($P<0.01$) increase in protein levels and 2.2-fold ($P<0.05$) increase in activity levels (Fig. 5A-C). In addition, we showed that malonyl-CoA did not inhibit CPT1 activity in CPT1AM-expressing macrophages (Fig. 5C). CPT1AM-expressing macrophages showed a 1.5-fold increase in FAO rate compared to GFP control cells (Fig. 5D, $P<0.05$) and a total restoration in palmitate-induced enhancement of TG content (Fig. 5E and F).

Enhanced macrophage FAO reduced inflammation, ER stress and ROS damage

Palmitate-induced increase in proinflammatory cytokines (TNF-α, MCP-1, IL-1β, TLR-4 and IL-12p40) and ER stress markers (CHOP, GRP78, PDI and EDEM)

501 mRNA and protein levels was blunted in CPT1AM-expressing macrophages (Fig. 6A,
502 B, D and E)). Consistent with previous studies (18, 47, 48), palmitate incubation raised
503 cytokines expression by 2-3-fold. No differences were seen in anti-inflammatory
504 markers such as IL-10, Mgl-1 and IL-4 in CPT1AM-expressing cells incubated with or
505 without palmitate (Fig. 6C). Incubation with etomoxir, a permanent inhibitor of CPT1A,
506 counteracted the reduction of MCP-1 expression seen in CPT1AM-expressing cells
507 incubated with palmitate (data not shown). We also studied the effect of enhanced FAO
508 in RAW 264.7 macrophages on palmitate-induced ROS damage by protein carbonyl
509 content analysis. Palmitate-induced ROS damage was reduced in CPT1AM-expressing
510 macrophages (Fig. 6F). This reduction was not detected when ROS (superoxide) was
511 directly measured by using the MitoSOX Red probe (Fig. 6G).
512

DISCUSSION

The obesity epidemic has put a spotlight on the adipose tissue as a key player in obesity-induced insulin resistance (38). Obese individuals and those with T2D have lower FAO rates (17, 19, 37). Although these data were reported in skeletal muscle, we expected to see reduced CPT1A expression levels in the adipose tissue of both obese and T2D patients. However, no differences were seen in CPT1A mRNA expression between the obese or T2D and their respective controls either in VAT or in SAT. Other authors have reported a decrease in VAT CPT1 mRNA and protein levels in obese individuals (20). However, the authors did not specify which of the CPT1 isoforms was measured in VAT: CPT1A or CPT1B. We showed that CPT1A expression is higher in adipose tissue macrophages than in mature adipocytes. Since the obese adipose tissue has higher infiltration of immune cells such as macrophages, we postulate that the putative decrement of CPT1A expression in obese individuals could be compensated by increased expression from the infiltrated macrophages and thus, no differences are seen between the groups. CPT1B isoform is also expressed in human adipose tissue and it has been shown to raise FAO in metabolic tissues such as skeletal muscle (3). Thus, we measured mRNA and protein levels in the obese and T2D cohorts. However, no differences were seen among the groups indicating that CPT1B expression is not changed by obesity and T2D.

We found that in insulin sensitive individuals (control and overweight patients from the obese cohort and control patients from the T2D cohort) CPT1A mRNA expression was higher in VAT than in SAT. However, no differences between VAT and SAT were seen in the more insulin-resistant individuals with a more pro-inflammatory environment: obese and T2D patients. A similar phenomenon was described for T regulatory cells, described to have anti-inflammatory properties and to improve obesity-

induced insulin resistance (7). The authors reported that VAT and SAT of healthy individuals had similar low numbers of T regulatory cells at birth, with a progressive accumulation over time in the VAT, though not the SAT. Our results suggest a CPT1A expression balance between SAT and VAT depots that may be disturbed in obese and T2D patients. The difference in CPT1A expression between these two fat depots is potentially crucial, given the association of VAT, but not SAT with insulin resistance (1, 52). It might indicate, in healthy individuals, a potential protective role of CPT1A in the more insulin-resistant associated VAT.

Gene expression analysis revealed a negative association between CPT1A and the adipocyte marker of differentiation PPAR-γ. This is consistent with the fact that while white adipocytes mature they shift their lipid preferences to storage rather than oxidation. Aging was associated with reduced CPT1A expression in VAT. This might reflect a potential protective role of CPT1A expression in VAT, which is lost with age. Considering that VAT accretion is a hallmark of aging and especially, it is a stronger risk factor for comorbidities and mortality (23), we speculate a favorable role of enhanced CPT1A expression in age metabolic decline and related pathological conditions. Positive correlation both in VAT and SAT CPT1A was found with AGPAT5, SREBF1, BCL2 and CD163. These results may indicate a potential role of CPT1A in lipid biosynthesis processes (AGPAT5), glucose and lipid metabolism (SREBF1) and in protecting adipose tissue from apoptosis (BCL2). The positive association between CPT1A and CD163 (macrophage marker) was not surprising given the higher CPT1A expression in macrophages than in adipocytes (Fig. 2).

We are aware that many of the above mentioned associations may be secondary to obesity or T2D and that no causal relationship may be inferred with this study design. In order to prove the causality of some of these observations we performed *in vitro*

563 studies directly targeting adipocytes and macrophages to burn off the excess lipids
564 through an increase in FAO. We used the high-infection efficiency adipocyte cell line,
565 3T3-L1 CARΔ1 (31), to express for the first time CPT1AM through adenoviral
566 infection. Noteworthy, white adipocytes are designed to store lipids rather than to
567 oxidize them. Thus, CPT1 activity in WAT is lower than in other tissues (6). However,
568 CPT1AM-expressing adipocytes showed a 4.3-fold increase in CPT1 activity that was
569 not inhibited despite incubation with high concentrations of malonyl-CoA. Since
570 increased lipid accumulation, inflammation, ER stress and ROS-induced protein
571 damage trigger metabolic diseases we decided to measure TG content, inflammation,
572 ER stress and ROS damage as important mechanisms that could explain the potential
573 protective effect of CPT1AM expression. Enhanced FAO led to complete restoration of
574 TG content, improved insulin signaling (measured as pAkt), increased IRbeta
575 expression and cell viability and reduced inflammation in palmitate-incubated
576 CPT1AM-expressing adipocytes. CPT1AM-expressing adipocytes showed a general
577 improvement in lipid-induced derangements as a consequence of increased FA flux
578 through mitochondria. However, enhanced FA flux in the absence of a concomitant
579 dissipation of FAO metabolites has been associated with increased ROS damage (35)
580 and inflammation (8, 21, 43). Interestingly, while no differences were seen in ER or
581 oxidative stress (data not shown), CPT1AM-expressing adipocytes showed a significant
582 decrease in proinflammatory mediators such as IL-1β and MCP-1. The favorable role of
583 CPT1A in adipocytes to attenuate FA evoked insulin resistance and inflammation has
584 been also described to act via suppression of JNK (9). These results suggest that factors
585 other than a FAO increase *per se* are responsible for ROS production and inflammation.
586 Accumulation of toxic substances (diacylglycerol or ceramides) (49), hypoxia (15), as
587 well as cytokines (42) might participate in the induction of ROS damage and the

588 inflammatory state. Several researchers have demonstrated that enhanced FAO through
589 CPT1A or CPT1AM expression results in a decrease in relevant lipid mediators
590 involved in inflammation and insulin resistance such as diacylglycerol, intracellular
591 NEFAs (non-esterified FA), free FA, ceramides and TG (3, 9, 13, 26, 29, 40, 45). While
592 some authors (3) didn't see changes in skeletal muscle acylcarnitines' profile our group
593 has shown an increase in several acylcarnitines in CPT1AM-expressing neurons (25).

594 FA undergoing β-oxidation yield acetyl-CoA moieties that have two main
595 possible fates: (1) entry to the Krebs cycle for complete oxidation and ATP production,
596 or (2) conversion to ketone bodies (mainly in the liver). We observed increased FAO to
597 CO_2 and acid soluble products in CPT1AM-expressing adipocytes and macrophages.
598 CPT1AM expression in liver has been shown to enhance ATP and ketone bodies
599 production with no changes in glucose oxidation (29), (13). Altogether, this indicates a
600 metabolic rate switch towards FA.

601 Monocytes were the first immune cells reported to infiltrate obese adipose
602 tissue, differentiate to macrophages, produce inflammatory cytokines and trigger insulin
603 resistance (56, 57). Thus, we examined whether CPT1AM expression could play a
604 protective role in obesity-induced macrophage derangements. We found that, in human
605 WAT, CPT1A is highly expressed in SVF compared to adipocytes. This happened both
606 in human VAT and SAT. A closer histological and immunofluorescence examination
607 showed that macrophages present in the adipose tissue expressed CPT1A. This does not
608 rule out CPT1A expression in other immune cells also present in the adipose tissue such
609 as T and B cells, T regulatory cells, and mast cells.

610 Given the high CPT1A expression in human adipose tissue macrophages, we
611 decided to study the effect of CPT1AM in RAW 264.7 macrophages. A permanently
612 enhanced FAO rate in CPT1AM-expressing macrophages led to a complete restoration

of palmitate-induced increase in TG content, and a decrease in inflammation, ER and oxidative stress without affecting cell viability. Recent data show that FAO is capable of regulating the degree of acyl chain saturation in ER phospholipids (28). Since increasing the degree of saturation in ER phospholipids has been described to directly activate ER stress and inflammation (28) this might provide a mechanistic link to how FAO alleviates ER stress under palmitate loading. Thus, enhancing CPT1A expression in macrophages may be a potential approach to fight against obesity-induced disorders.

In conclusion, we have shown that CPT1A expression was higher in human adipose tissue macrophages than in mature adipocytes and that it was differentially expressed in VAT *vs.* SAT. Further *in vitro* studies demonstrated that an increase in FAO in lipid-treated adipocytes and macrophages reduced TG content and inflammatory levels, improved insulin sensitivity in adipocytes, and reduced ER stress and ROS damage in macrophages. Adipocyte specific knockout or transgenic animal models for CPT1A would be especially relevant to elucidate its potential protection against obesity-induced insulin resistance *in vivo*. Our data support the hypothesis that pharmacological or genetic strategies to enhance FAO may be beneficial for the treatment of chronic inflammatory pathologies such as obesity and T2D.

Funding

This study was supported by the Spanish Ministry of Science and Innovation (Grants SAF2010-20039 and SAF2013-45887-R to LH, SAF2011-30520-C02-01 to DS, PI11/00085 to JJV, SAF2012-33014 to BP, SAF2012-36186 to SF-V, SAF2012-30708 to MVC, SAF2011-23626 to FV and doctoral fellowships to MIM and JFM), by the CIBER Fisiopatología de la Obesidad y la Nutrición (CIBERobn) (Grant CB06/03/0001 to DS) and CIBER Diabetes y Enfermedades Metabólicas Asociadas (CIBERDEM) (Grant CB07/08/0003 to MVC), Instituto de Salud Carlos III, by the European Union (BetaBat project FP7-277713 to FV), by the European Foundation for the Study of Diabetes (EFSD)/Lilly and EFSD/Janssen-Rising Star research fellowships to LH and by the L'Oréal-UNESCO "For Women in Science" research fellowship to LH. MW is a recipient of the Ciência sem Fronteiras-CNPq fellowship (237976/2012-9).

Acknowledgements

We thank Professor F.G. Hegardt and Dr. G. Asins for helpful comments and suggestions, A. Orozco for technical assistance and R. Rycroft from the Language Service of the University of Barcelona for valuable assistance in the preparation of the English manuscript. We also thank D. Orlicky for kindly providing 3T3-L1 CARΔ1 adipocytes. SF-V acknowledges support from the "Miguel Servet" tenure track program (CP10/00438) from the Fondo de Investigación Sanitaria (FIS) and co-financed by the European Regional Development Fund (ERDF).

Contribution statement

All the authors contributed to the conception and design of the study. MIM, RF, MW, MCD, JFM, LV, XE, MG-S, BP and LS carried out the experiments. All authors

contributed to the analysis and interpretation of data and revising it critically for important intellectual content. MIM, RF, MCD, JFM, BP, JJV and LH wrote the manuscript. All authors revised and approved the final manuscript.

663 **REFERENCES**

664 1. **Bosello O, Zamboni M**. Visceral obesity and metabolic syndrome. *Obes Rev* 1:
665 47–56, 2000.

666 2. **Brown NF, Hill JK, Esser V, Kirkland JL, Corkey BE, Foster DW, Garry**
667 **JDMC**. Mouse white adipocytes and 3T3-L1 cells display an anomalous pattern
668 of carnitine palmitoyltransferase (CPT) I isoform expression during
669 differentiation. *Biochem J* 231: 225–231, 1997.

670 3. **Bruce CR, Hoy AJ, Turner N, Watt MJ, Allen TL, Carpenter K, Cooney**
671 **GJ, Febbraio M a, Kraegen EW**. Overexpression of carnitine
672 palmitoyltransferase-1 in skeletal muscle is sufficient to enhance fatty acid
673 oxidation and improve high-fat diet-induced insulin resistance. *Diabetes* 58: 550–
674 8, 2009.

675 4. **Bruce CR, Hoy AJ, Turner N, Watt MJ, Allen TL, Carpenter K, Cooney**
676 **GJ, Febbraio MA, Kraegen EW**. Overexpression of carnitine
677 palmitoyltransferase-1 in skeletal muscle is sufficient to enhance fatty acid
678 oxidation and improve high-fat diet-induced insulin resistance. *Diabetes* 58: 550–
679 8, 2009.

680 5. **Davies LC, Jenkins SJ, Allen JE, Taylor PR**. Tissue-resident macrophages.
681 *Nat Immunol* 14: 986–95, 2013.

682 6. **Doh K-O, Kim Y-W, Park S-Y, Lee S-K, Park JS, Kim J-Y**. Interrelation
683 between long-chain fatty acid oxidation rate and carnitine palmitoyltransferase 1
684 activity with different isoforms in rat tissues. *Life Sci* 77: 435–43, 2005.

685 7. **Feuerer M, Herrero L, Cipolletta D, Naaz A, Wong J, Nayer A, Lee J,**
686 **Goldfine AB, Benoist C, Shoelson S, Mathis D**. Lean, but not obese, fat is
687 enriched for a unique population of regulatory T cells that affect metabolic
688 parameters. *Nat Med* 15: 930–939, 2009.

689 8. **Furukawa S, Fujita T, Shimabukuro M, Iwaki M, Yamada Y, Nakajima Y,**
690 **Nakayama O, Makishima M, Matsuda M, Shimomura I**. Increased oxidative
691 stress in obesity and its impact on metabolic syndrome. *J Clin Invest* 114: 1752–
692 1761, 2004.

693 9. **Gao X, Li K, Hui X, Kong X, Sweeney G, Wang Y, Xu A, Teng M, Liu P,**
694 **Wu D**. Carnitine palmitoyltransferase 1A prevents fatty acid-induced adipocyte
695 dysfunction through suppression of c-Jun N-terminal kinase. *Biochem J* 435:
696 723–732, 2011.

697 10. **Gesta S, Bezy O, Mori MA, Macotela Y, Lee KY, Kahn CR**. Mesodermal
698 developmental gene Tbx15 impairs adipocyte differentiation and mitochondrial
699 respiration. *Proc Natl Acad Sci U S A* 108: 2771–6, 2011.

11. **Hamada Y, Nagasaki H, Fujiya A, Seino Y, Shang Q-L, Suzuki T, Hashimoto H, Oiso Y**. Involvement of de novo ceramide synthesis in pro-inflammatory adipokine secretion and adipocyte-macrophage interaction. *J Nutr Biochem* 25: 1309–16, 2014.

12. **Haslam DW, James WPT**. Obesity. *Lancet* 366: 1197–1209, 2005.

13. **Herrero L, Rubí B, Sebastián D, Serra D, Asins G, Maechler P, Prentki M, Hegardt FG**. Alteration of the malonyl-CoA/carnitine palmitoyltransferase I interaction in the beta-cell impairs glucose-induced insulin secretion. *Diabetes* 54: 462–471, 2005.

14. **Herrero L, Shapiro H, Nayer A, Lee J, Shoelson SE**. Inflammation and adipose tissue macrophages in lipodystrophic mice. *Proc Natl Acad Sci U S A* 107: 240–245, 2010.

15. **Hosogai N, Fukuhara A, Oshima K, Miyata Y, Tanaka S, Segawa K, Furukawa S, Tochino Y, Komuro R, Matsuda M, Shimomura I**. Adipose tissue hypoxia in obesity and its impact on adipocytokine dysregulation. *Diabetes* 56: 901–911, 2007.

16. **Hotamisligil GS**. Endoplasmic reticulum stress and the inflammatory basis of metabolic disease. *Cell* 140: 900–17, 2010.

17. **Houmard JA**. Intramuscular lipid oxidation and obesity. *Am J Physiol Regul Integr Comp Physiol* 294: R1111–1116, 2008.

18. **Huang S, Rutkowsky JM, Snodgrass RG, Ono-Moore KD, Schneider DA, Newman JW, Adams SH, Hwang DH**. Saturated fatty acids activate TLR-mediated proinflammatory signaling pathways. *J Lipid Res* 53: 2002–13, 2012.

19. **Kelley DE, He J, Menshikova E V, Ritov VB**. Dysfunction of Mitochondria in Human Skeletal Muscle in Type 2 Diabetes. *Diabetes* 51: 2944–2950, 2002.

20. **Krishnan J, Danzer C, Simka T, Ukropec J, Walter KM, Kumpf S, Mirtschink P, Ukropcova B, Gasperikova D, Pedrazzini T, Krek W**. Dietary obesity-associated Hif1α activation in adipocytes restricts fatty acid oxidation and energy expenditure via suppression of the Sirt2-NAD+ system. *Genes Dev* 26: 259–70, 2012.

21. **Lin Y, Berg AH, Iyengar P, Lam TK, Giacca A, Combs TP, Rajala MW, Du X, Rollman B, Li W, Hawkins M, Barzilai N, Rhodes CJ, Fantus IG, Brownlee M, Scherer PE**. The hyperglycemia-induced inflammatory response in adipocytes: the role of reactive oxygen species. *J Biol Chem* 280: 4617–4626, 2005.

22. **Mathis D**. Immunological goings-on in visceral adipose tissue. *Cell Metab* 17: 851–9, 2013.

23. **Matsuzawa Y, Shimomura I, Nakamura T, Keno Y, Tokunaga K**. Pathophysiology and pathogenesis of visceral fat obesity. *Ann N Y Acad Sci* 748: 399–406, 1995.

24. **Matthews DR, Hosker JP, Rudenski AS, Naylor BA, Treacher DF, Turner RC**. Homeostasis model assessment: insulin resistance and beta-cell function from fasting plasma glucose and insulin concentrations in man. *Diabetologia* 28: 412–419, 1985.

25. **Mera P, Mir JF, Fabriàs G, Casas J, Costa ASH, Malandrino MI, Fernández-López J-A, Remesar X, Gao S, Chohnan S, Rodríguez-Peña MS, Petry H, Asins G, Hegardt FG, Herrero L, Serra D**. Long-term increased carnitine palmitoyltransferase 1A expression in ventromedial hypotalamus causes hyperphagia and alters the hypothalamic lipidomic profile. *PLoS One* 9: e97195, 2014.

26. **Monsénégo J, Mansouri A, Akkaoui M, Lenoir V, Esnous C, Fauveau V, Tavernier V, Girard J, Prip-Buus C**. Enhancing liver mitochondrial fatty acid oxidation capacity in obese mice improves insulin sensitivity independently of hepatic steatosis. *J Hepatol* 56: 632–639, 2012.

27. **Morillas M, Gómez-Puertas P, Bentebibel A, Sellés E, Casals N, Valencia A, Hegardt FG, Asins G, Serra D**. Identification of conserved amino acid residues in rat liver carnitine palmitoyltransferase I critical for malonyl-CoA inhibition. Mutation of methionine 593 abolishes malonyl-CoA inhibition. *J Biol Chem* 278: 9058–63, 2003.

28. **Namgaladze D, Lips S, Leiker TJ, Murphy RC, Ekroos K, Ferreiros N, Geisslinger G, Brüne B**. Inhibition of macrophage fatty acid β-oxidation exacerbates palmitate-induced inflammatory and endoplasmic reticulum stress responses. *Diabetologia* 57: 1067–1077, 2014.

29. **Orellana-Gavalda JM, Herrero L, Malandrino MI, Paneda A, Sol Rodriguez-Pena M, Petry H, Asins G, Van Deventer S, Hegardt FG, Serra D**. Molecular therapy for obesity and diabetes based on a long-term increase in hepatic fatty-acid oxidation. *Hepatology* 53: 821–832, 2011.

30. **Orellana-Gavaldà JM, Herrero L, Malandrino MI, Pañeda A, Sol Rodríguez-Peña M, Petry H, Asins G, Van Deventer S, Hegardt FG, Serra D**. Molecular therapy for obesity and diabetes based on a long-term increase in hepatic fatty-acid oxidation. *Hepatology* 53: 821–832, 2011.

31. **Orlicky DJ, DeGregori J, Schaack J**. Construction of stable coxsackievirus and adenovirus receptor-expressing 3T3-L1 cells. *J Lipid Res* 42: 910–915, 2001.

32. **Patti M-E, Corvera S**. The role of mitochondria in the pathogenesis of type 2 diabetes. *Endocr Rev* 31: 364–95, 2010.

33. **Perdomo G, Commerford SR, Richard A-MT, Adams SH, Corkey BE, O'Doherty RM, Brown NF**. Increased beta-oxidation in muscle cells enhances

insulin-stimulated glucose metabolism and protects against fatty acid-induced insulin resistance despite intramyocellular lipid accumulation. *J Biol Chem* 279: 27177–27186, 2004.

34. **Pérez-Pérez R, García-Santos E, Ortega-Delgado FJ, López JA, Camafeita E, Ricart W, Fernández-Real J-M, Peral B**. Attenuated metabolism is a hallmark of obesity as revealed by comparative proteomic analysis of human omental adipose tissue. *J Proteomics* 75: 783–95, 2012.

35. **Pessayre D, Fromenty B, Mansouri A**. Mitochondrial injury in steatohepatitis. *Eur J Gastroenterol Hepatol* 16: 1095–1105, 2004.

36. **Price N, van der Leij F, Jackson V, Corstorphine C, Thomson R, Sorensen A, Zammit V**. A novel brain-expressed protein related to carnitine palmitoyltransferase I. *Genomics* 80: 433–442, 2002.

37. **Ritov VB, Menshikova E V, He J, Ferrell RE, Goodpaster BH, Kelley DE**. Deficiency of Subsarcolemmal Mitochondria in Obesity and Type 2 Diabetes. *Diabetes* 54: 8–14, 2004.

38. **Rosen ED, Spiegelman BM**. What We Talk About When We Talk About Fat. *Cell* 156: 20–44, 2014.

39. **Samuel VT, Shulman GI**. Mechanisms for insulin resistance: common threads and missing links. *Cell* 148: 852–71, 2012.

40. **Sebastian D, Herrero L, Serra D, Asins G, Hegardt FG**. CPT I overexpression protects L6E9 muscle cells from fatty acid-induced insulin resistance. *Am J Physiol Endocrinol Metab* 292: E677–86, 2007.

41. **Sebastián D, Herrero L, Serra D, Asins G, Hegardt FG**. CPT I overexpression protects L6E9 muscle cells from fatty acid-induced insulin resistance. *Am J Physiol Endocrinol Metab* 292: E677–86, 2007.

42. **Shoelson SE, Herrero L, Naaz A**. Obesity, inflammation, and insulin resistance. *Gastroenterology* 132: 2169–80, 2007.

43. **Shoelson SE, Lee J, Goldfine AB**. Inflammation and insulin resistance. *J Clin Invest* 116: 1793–1801, 2006.

44. **Simoneau JA, Veerkamp JH, Turcotte LP, Kelley DE**. Markers of capacity to utilize fatty acids in human skeletal muscle: relation to insulin resistance and obesity and effects of weight loss. *FASEB J* 13: 2051–60, 1999.

45. **Stefanovic-Racic M, Perdomo G, Mantell BS, Sipula IJ, Brown NF, O'Doherty RM**. A moderate increase in carnitine palmitoyltransferase 1a activity is sufficient to substantially reduce hepatic triglyceride levels. *Am J Physiol Endocrinol Metab* 294: E969–77, 2008.

46. **Stefanovic-Racic M, Perdomo G, Mantell BS, Sipula IJ, Brown NF, O'Doherty RM**. A moderate increase in carnitine palmitoyltransferase 1a activity is sufficient to substantially reduce hepatic triglyceride levels. *Am J Physiol Endocrinol Metab* 294: E969–977, 2008.

47. **Suganami T, Nishida J, Ogawa Y**. A paracrine loop between adipocytes and macrophages aggravates inflammatory changes: role of free fatty acids and tumor necrosis factor alpha. *Arterioscler Thromb Vasc Biol* 25: 2062–8, 2005.

48. **Suganami T, Tanimoto-Koyama K, Nishida J, Itoh M, Yuan X, Mizuarai S, Kotani H, Yamaoka S, Miyake K, Aoe S, Kamei Y, Ogawa Y**. Role of the Toll-like receptor 4/NF-kappaB pathway in saturated fatty acid-induced inflammatory changes in the interaction between adipocytes and macrophages. *Arterioscler Thromb Vasc Biol* 27: 84–91, 2007.

49. **Summers SA**. Ceramides in insulin resistance and lipotoxicity. *Prog Lipid Res* 45: 42–72, 2006.

50. **Sun K, Kusminski CM, Scherer PE**. Review series Adipose tissue remodeling and obesity. 121, 2011.

51. **Sun K, Wernstedt Asterholm I, Kusminski CM, Bueno AC, Wang Z V, Pollard JW, Brekken R a, Scherer PE**. Dichotomous effects of VEGF-A on adipose tissue dysfunction. *Proc Natl Acad Sci U S A* 109: 5874–5879, 2012.

52. **Tran TT, Yamamoto Y, Gesta S, Kahn CR**. Beneficial effects of subcutaneous fat transplantation on metabolism. *Cell Metab* 7: 410–420, 2008.

53. **Villarroya F, Domingo P, Giralt M**. Lipodystrophy in HIV 1-infected patients: lessons for obesity research. *Int J Obes (Lond)* 31: 1763–76, 2007.

54. **Virtue S, Vidal-Puig A**. Adipose tissue expandability, lipotoxicity and the Metabolic Syndrome--an allostatic perspective. *Biochim Biophys Acta* 1801: 338–49, 2010.

55. **Wabitsch M, Brenner RE, Melzner I, Braun M, Moller P, Heinze E, Debatin KM, Hauner H**. Characterization of a human preadipocyte cell strain with high capacity for adipose differentiation. *Int J Obes Relat Metab Disord* 25: 8–15, 2001.

56. **Weisberg SP, McCann D, Desai M, Rosenbaum M, Leibel RL, Ferrante AW**. Obesity is associated with macrophage accumulation in adipose tissue. *J Clin Invest* 112: 1796–1808, 2003.

57. **Xu H, Barnes GT, Yang Q, Tan G, Yang D, Chou CJ, Sole J, Nichols A, Ross JS, Tartaglia LA, Chen H**. Chronic inflammation in fat plays a crucial role in the development of obesity-related insulin resistance. *J Clin Invest* 112: 1821–1830, 2003.

Tables

Table 1. Clinical, analytical and CPT1A gene expression analysis of the obesity cohort. BMI: Body mass index; sIL-6: soluble Interleukine-6; SBP: systolic blood pressure; DBP: Diastolic blood pressure. Values are expressed as mean ± SD or median (interquartile range) for a non-Gaussian distributed variables. Differences *vs.* Lean: *P<0.001; ¶P<0.05. Differences *vs.* Overweight: #P<0.001; §P<0.05. †P<0.05 SAT *vs.* VAT expression.

Table 2. Clinical, analytical and CPT1A gene expression analysis of the T2D cohort. BMI: Body mass index; sIL-6: soluble Interleukine-6; SBP: systolic blood pressure; DBP: Diastolic blood pressure. Values are expressed as mean ± SD or median (interquartile range) for a non-Gaussian distributed variables. Differences *vs*. controls: *P<0.001; ¶P<0.05. Differences between SAT and VAT in the same group: †P=0.03.

Table 3. Bivariate correlation analysis of CPT1A gene expression levels with several genes in human VAT and SAT of the obesity cohort. PPAR-γ, Peroxisome proliferator-activated receptor gamma; AGPAT5, 1-acylglycerol-3-phosphate O-acyltransferase 5; SREBF1, sterol regulatory element binding transcription factor 1; BCL2, B-cell CLL/lymphoma 2; CD163, macrophage and monocyte marker; p<0.005 for all correlations.

Table 4. Multiple regression analysis for CPT1A in VAT and SAT as dependent variable in the obesity cohort. Independent variables included in the model: age, gender, body mass index (BMI), peroxisome proliferator-activated receptor alpha (PPAR-α), peroxisome proliferator-activated receptor gamma (PPAR-γ), 1-acylglycerol-3-

876 phosphate O-acyltransferase 5 (AGPAT5), sterol regulatory element binding
877 transcription factor 1 (SREBF1), B-cell CLL/lymphoma 2 (BCL2) and macrophage and
878 monocyte marker (CD163) gene expression levels. β st: standardized beta coefficient.
879 CI: Confidence Interval.
880

881 **Figure legends**

882 **Fig. 1.** CPT1 gene and protein expression in human adipose tissue. (**A**, **B**) CPT1A
883 relative mRNA levels in human VAT and SAT of the obesity (A) or the T2D (B**)**
884 cohort. Number of individuals: 19 lean, 28 overweight, 15 obese, 36 control and 11
885 T2D (See Table 1 and 2 for more details). (**C, D**) CPT1A protein levels in human VAT
886 and SAT of seven lean individuals (P1-P7) (C) and three obese individuals (D). (**E, F**)
887 CPT1B relative mRNA levels in human VAT and SAT of the obesity (E) or the T2D
888 (F) cohort. *P<0.05.

889

890 **Fig. 2.** CPT1A is highly expressed in human adipose tissue macrophages. (**A**) CPT1A
891 mRNA levels in both adipose (AD) and stromal-vascular fraction (SVF) of human VAT
892 and SAT. n=4. *P<0.05. (**B**) Immunohistochemical detection of CPT1A (brown) in
893 SAT of obese subjects. (**C**) Immunofluorescence staining of CPT1A (red) and CD68
894 (green) proteins in SAT of obese individuals. The counterstaining of nuclei (DAPI) is
895 shown in blue. Images are representative of adipose tissue preparations collected from
896 three subjects.

897

898 **Fig. 3.** Adenovirus infection efficiency and viability in 3T3-L1 CARΔ1 adipocytes and
899 RAW 264.7 macrophages. Images were taken from (**A**) AdGFP-infected 3T3-L1
900 CARΔ1 adipocytes (50% infection) or (**B**) RAW 264.7 macrophages (70% infection)
901 48h or 72h after the infection, respectively. (**C**, **D**) Cell viability of (C) 3T3-L1 CARΔ1
902 adipocytes or (D) RAW 264.7 macrophages infected with AdGFP or AdCPT1AM and
903 incubated for 24h with 1mM or 0.3mM palmitate (PA), respectively.

904

905 **Fig. 4** Enhanced FAO in 3T3-L1 CARΔ1 adipocytes improves lipid-induced TG
906 accumulation, insulin sensitivity and inflammation. Relative CPT1A mRNA expression
907 (**A**) and protein levels (**B**) in AdGFP- or AdCPT1AM-infected 3T3-L1 CARΔ1
908 adipocytes. (**C**) CPT1 activity from mitochondria-enriched cell fractions incubated (or
909 not) with 100 μM malonyl-CoA. (**D**) Total FAO rate represented as the sum of acid
910 soluble products plus CO_2 oxidation. (**E**) TG content of adipocytes treated for 24 h with
911 1mM palmitate (PA). (**F**) Insulin signaling in GFP- and CPT1AM-expressing
912 adipocytes incubated with 0.3mM PA for 24 h as indicated by Western blotting of
913 insulin-induced Akt phosphorylation (pAkt) and IRbeta. (**G**) Quantification of pAkt
914 normalized by total Akt (fold change of arbitrary units, A.U.). (**H**) Quantification of
915 IRbeta normalized by β-actin. (**I, J**) Relative mRNA expression from GFP- or CPT1A-
916 expressing adipocytes incubated with 1mM PA for 24 h. (**K**) Protein levels of IL-1α in
917 the culture media of GFP- or CPT1A-expressing adipocytes incubated with 1mM PA
918 for 6 h. Shown representative experiments out of 3. n=3-6. *P<0.05.
919
920 **Fig. 5.** Enhanced FAO and reduced TG content in CPT1AM-expressing RAW 264.7
921 macrophages. Relative CPT1A mRNA expression (**A**) and protein levels (**B**) in AdGFP-
922 or AdCPT1AM-infected macrophages. (**C**) CPT1 activity from mitochondria-enriched
923 cell fractions incubated (or not) with 100 μM malonyl-CoA. (**D**) Total FAO rate
924 measured as the sum of acid soluble products plus CO_2 oxidation. (**E**) TG content and
925 (**F**) Oil Red O staining of macrophages treated for 18 h with 0.75 mM palmitate (PA).
926 Shown representative experiments out of 3. n=3-6. *P<0.05.
927
928 **Fig. 6.** CPT1AM expression reduced inflammation, ER stress and ROS damage in
929 RAW 264.7 macrophages. (**A**, **C, D**) Relative mRNA gene expression from

macrophages incubated with 0.5 mM palmitate (PA) for 8 h (TNF-α and MCP-1) or 0.3 mM PA for 24 h (IL-10, Mgl-1, IL-4, IL-1β, TLR-4, CHOP, GRP78, PDI and EDEM). (**B**) Protein levels of IL-12p40 in the culture media of macrophages incubated with 0.3 mM PA for 24 h. (**E**) CHOP protein levels and quantification in macrophages incubated with 0.5 mM PA for 8 h (**F**) Protein carbonyl content analysis and quantification in macrophages incubated with 0.75 mM PA for 18 h. (**G**) Measurement of ROS (superoxide) using the MitoSOX Red probe. Shown representative experiments out of 3. n=3-4 *P<0.05.

Table 1

	Lean **BMI<25** (13 male; 6 female)	**Overweight** **25=<BMI<30** (16 male; 12 female)	**Obese** **BMI>=30** (9 male; 6 female)
Age (years)	51.7 ± 16.0	57.1 ± 15.0	57.4 ± 12.8
BMI (kg/m^2)	23.6 (22.1-24.2)	27.2 (26.5-27.9)*	32.1 (30.8-33.6)*#
Waist (cm)	83.0 (79.0-90.0)	97.0 (90.5-100.0)*	107.0 (100.0-117.2)*#
Cholesterol (mM)	5.2 ± 1.2	4.9 ± 1.0	5.2 ± 0.8
HDL-chol (mM)	1.5 ± 0.5	1.3 ± 0.3	1.4 ± 0.3
Triglycerides (mM)	1.0 (0.7-1.6)	1.1 (0.8-1.5)	1.0 (0.7-1.3)
Glucose (mM)	4.8 ± 0.7	5.5 ± 0.5*	5.6 ± 0.5*
Insulin (μIU/ml)	3.4 (2.1-6.7)	4.0 (2.8-7.2)	6.6 (4.5-16.5)¶
HOMA-IR	0.75 (0.54-1.83)	1.01 (0.52-2.09)	1.60 (1.19-4.79) ¶
sIL-6 (pg/ml)	1.4 (1.1-2.5)	1.0 (0.7-2.2)	2.5 (1.4-5.2) §
SBP (mmHg)	120 (120-127)	130 (121-140)	145 (130-160)*§
DBP (mmHg)	70 (60-80)	70 (70-80)	80 (78-90)¶
SAT *CPT1A*	0.85 (0.66-1.14)†	1.15 (0.85-1.60) †	0.86 (0.72-1.81)
VAT *CPT1A*	1.31 (1.07-2.50)	1.42 (0.97-3.00)	1.07 (0.84-1.76)

Table 2

	Control (21 male, 15 female)	**Type2 Diabetes** (5 male, 6 female)
Age (years)	61.6 ± 10.6	66.1± 8.6
BMI (kg/m^2)	28.6 (27.0 -31.5)	28.7 (26.9 -30.4)
Waist (cm)	100.0 (94.0 -107.0)	97.0 (94.0 -102.0)
Cholesterol (mM)	5.1 ± 0.9	4.7 ± 1.2
HDL-chol (mM)	1.4 (1.2 -1.6)	1.2 (1.0 -1.9)
Triglycerides (mM)	1.0 (0.7 -1.5)	1.7 (1.2 -2.3) ¶
NEFA (μM)	775.5 ± 275.1	926.4 ± 412.3
Glycerol (μM)	135.2 (117.2 -222.3)	301.6 (209.6 -465.3) ¶
Glucose (mM)	5.6 (5.3 -5.8)	8.3 (7.0 -10.1)*
Insulin (μIU/ml)	4.5 (3.5 -7.7)	10.2 (3.5 -21.4)
HOMA -IR	1.22 (0.89 -2.10)	3.66 (1.71 -23.66) ¶
sIL-6 (pg/ml)	1.4 (1.0 -2.6)	1.5 (1.0 -2.4)
SBP (mmHg)	140 (130 -150)	140 (124 -156)
DBP (mmHg)	80 (70 -80)	80(63 -83)
SAT *CPT1A*	1.08 (0.79 -1.59) †	1.70 (1.03 -2.18)
VAT *CPT1A*	1.39 (0.87 -2.28)	1.57 (0.98 -1.96)

Table 3

	CPT1A	
	SAT **R**	VAT **R**
PPAR-γ	-0.382	
AGPAT5	0.639	0.714
SREBF1	0.525	0.757
BCL2	0.639	0.580
CD163	0.731	0.716

Table 4

SAT (R^2 of the model: 0.71)

Independent variables	B (95% CI)	β st	*p*
CD163	0.34 (0.20 – 0.49)	0.446	<0.0001
AGPAT5	0.64 (0.33 – 0.95)	0.345	<0.0001
SREBF1	0.19 (0.06 – 0.33)	0.245	0.006

VAT (R^2 of the model: 0.70)

Independent variables	B (95% CI)	β st	*p*
CD163	0.34 (0.21 – 0.48)	0.569	<0.0001
Age	-0.15 (-0-025 – -0.004)	-0.22	0.006
SREBF1	0.413 (0.13 – 0.69)	0.323	0.005
PPAR-γ	-0.29 (-0.53 – -0.05)	-0.19	0.017

Figure 1

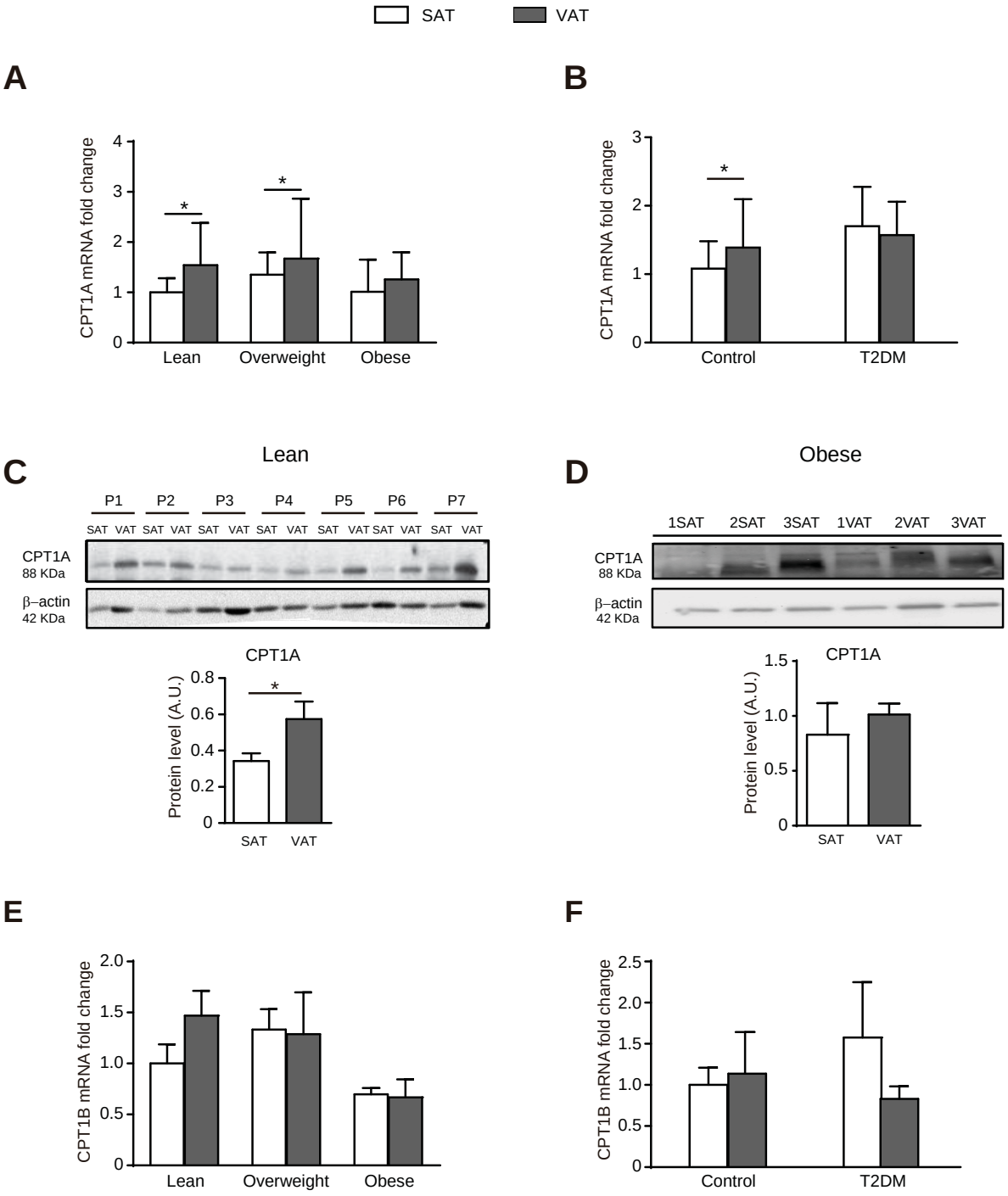
SAT
VAT
A
CPT1A mRNA fold change
Lean
Overweight
Obese
B
CPT1A mRNA fold change
Control
T2DM
C
Lean
P1 P2 P3 P4 P5 P6 P7
SAT VAT SAT VAT SAT VAT SAT VAT SAT VAT SAT VAT SAT VAT
CPT1A
88 KDa
β–actin
42 KDa
CPT1A
Protein level (A.U.)
SAT
VAT
D
Obese
1SAT 2SAT 3SAT 1VAT 2VAT 3VAT
CPT1A
88 KDa
β–actin
42 KDa
CPT1A
Protein level (A.U.)
SAT
VAT
E
CPT1B mRNA fold change
Lean
Overweight
Obese
F
CPT1B mRNA fold change
Control
T2DM

Figure 2

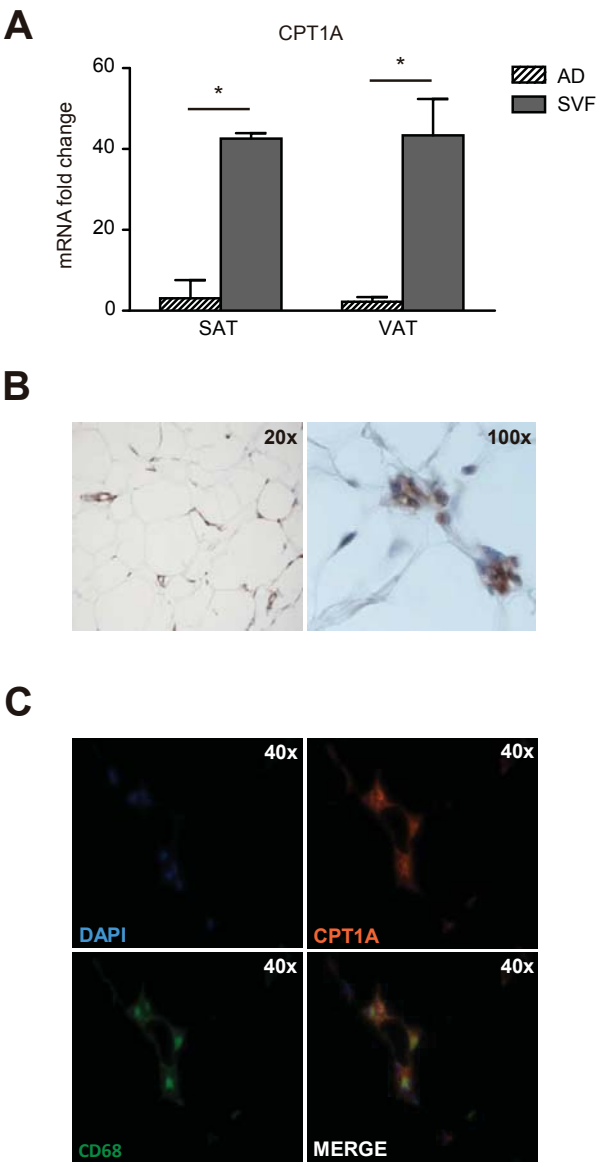
A
CPT1A
mRNA fold change
60
40
20
0
*
*
AD
SVF
SAT
VAT
B
20x
100x
C
40x
DAPI
40x
CPT1A
40x
CD68
40x
MERGE

Figure 3

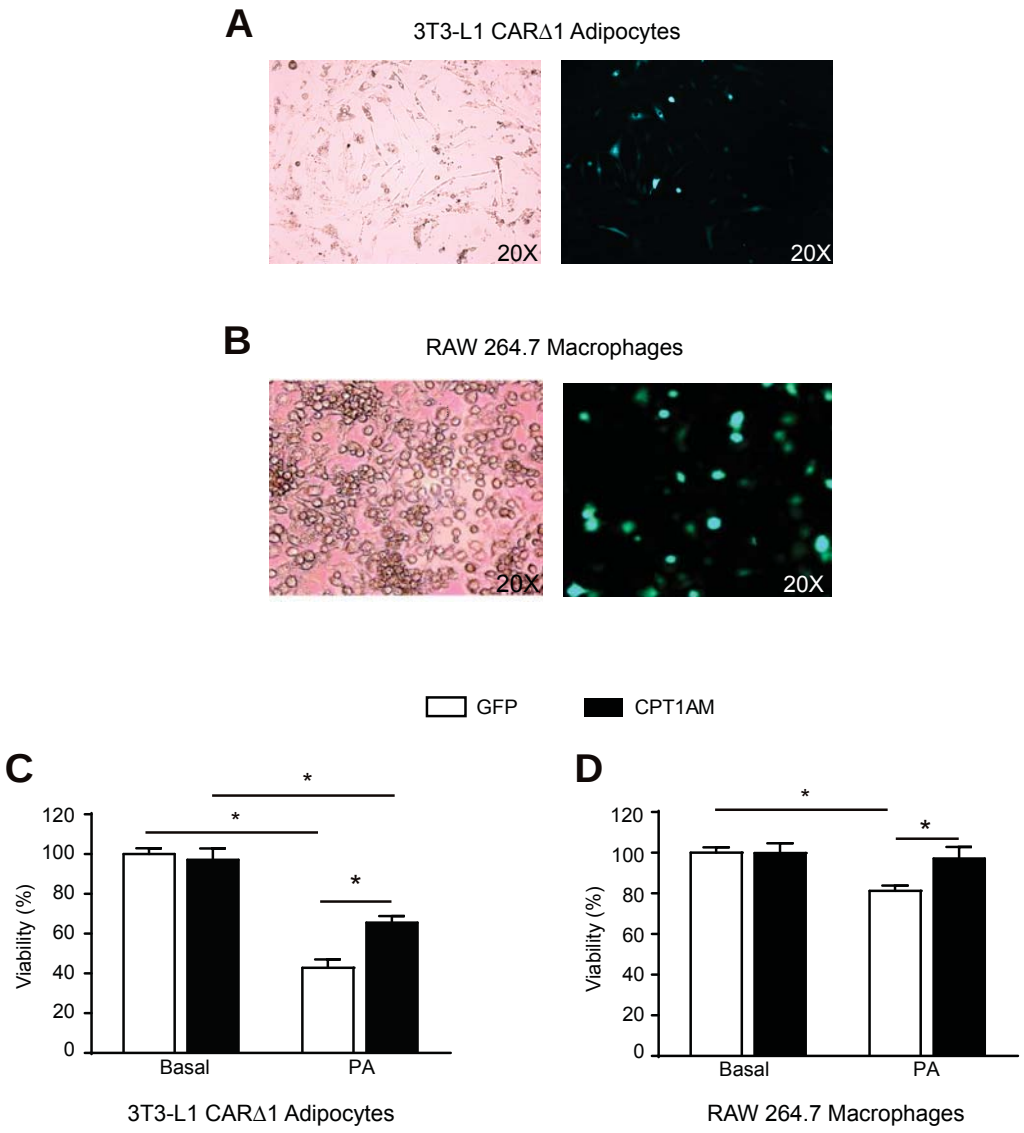
A
3T3-L1 CARΔ1 Adipocytes
20X
20X
B
RAW 264.7 Macrophages
20X
20X
GFP
CPT1AM
C
Viability (%)
120
100
80
60
40
20
0
Basal
PA
3T3-L1 CARΔ1 Adipocytes
D
Viability (%)
120
100
80
60
40
20
0
Basal
PA
RAW 264.7 Macrophages

Figure 4

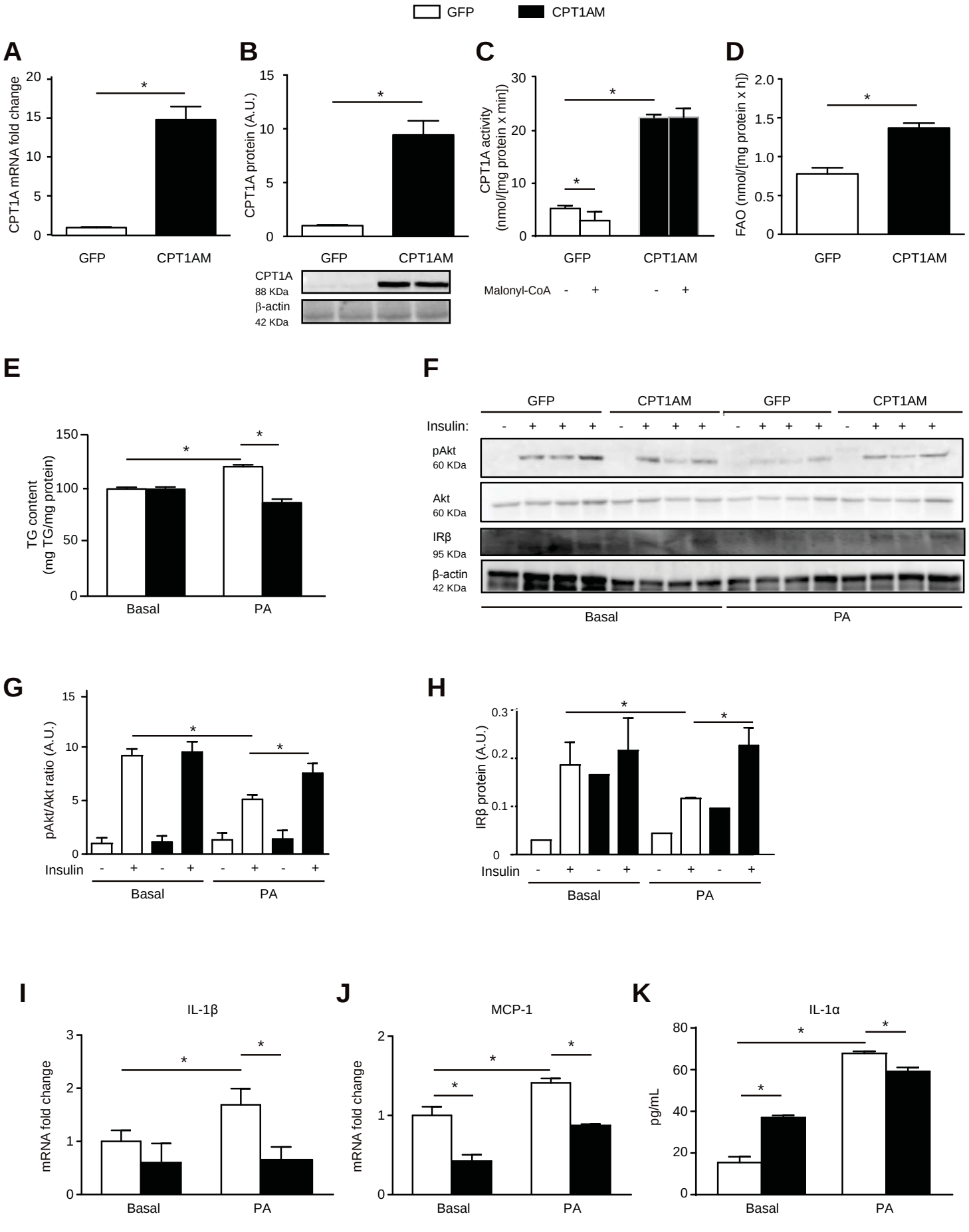
GFP
CPT1AM
A
CPT1A mRNA fold change
B
CPT1A protein (A.U.)
CPT1A
88 KDa
β-actin
42 KDa
C
CPT1A activity (nmol/[mg protein x min])
Malonyl-CoA
D
FAO (nmol/[mg protein x h])
E
TG content (mg TG/mg protein)
Basal
PA
F
Insulin:
pAkt
60 KDa
Akt
60 KDa
IRβ
95 KDa
β-actin
42 KDa
G
pAkt/Akt ratio (A.U.)
H
IRβ protein (A.U.)
I
IL-1β
mRNA fold change
J
MCP-1
K
IL-1α
pg/mL

Figure 5

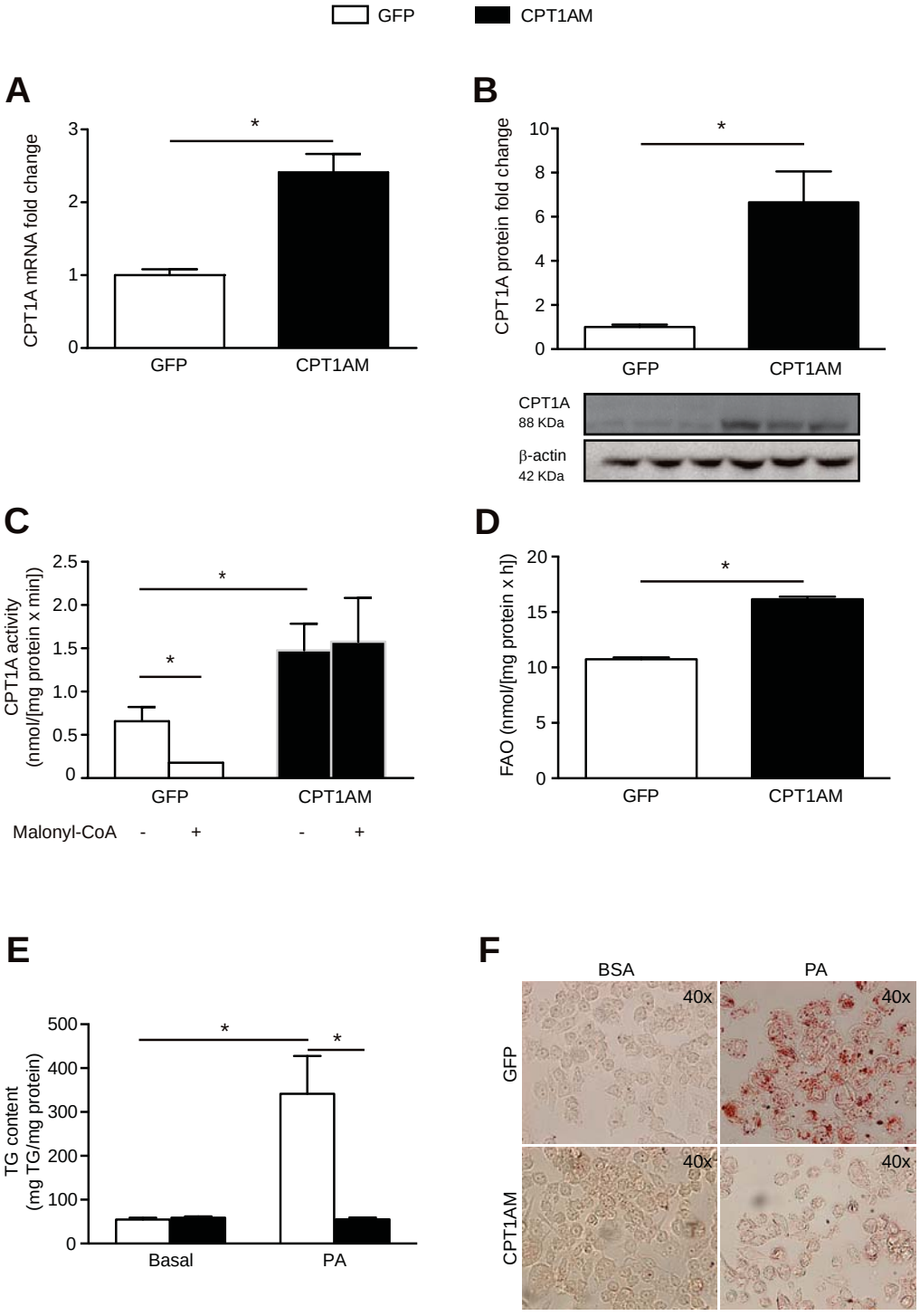
GFP
CPT1AM
A
CPT1A mRNA fold change
3
2
1
0
*
GFP
CPT1AM
B
CPT1A protein fold change
10
8
6
4
2
0
*
GFP
CPT1AM
CPT1A
88 KDa
β-actin
42 KDa
C
CPT1A activity
(nmol/[mg protein x min])
2.5
2.0
1.5
1.0
0.5
0
*
*
GFP
CPT1AM
Malonyl-CoA - + - +
D
FAO (nmol/[mg protein x h])
20
15
10
5
0
*
GFP
CPT1AM
E
TG content
(mg TG/mg protein)
500
400
300
200
100
0
*
*
Basal
PA
F
BSA
PA
GFP
CPT1AM
40x
40x
40x
40x

Figure 6

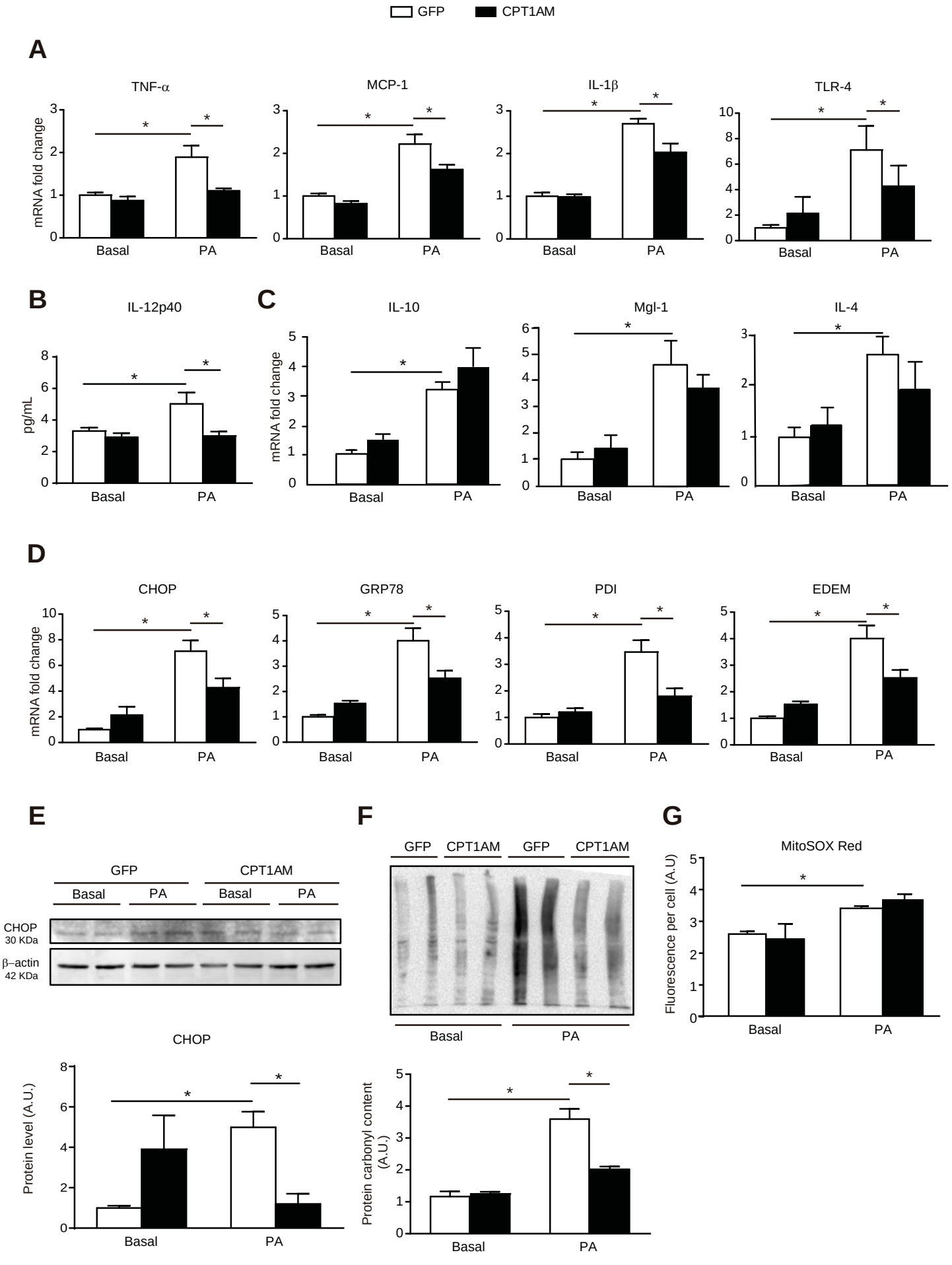
GFP
CPT1AM
A
TNF-α
MCP-1
IL-1β
TLR-4
mRNA fold change
Basal
PA
B
IL-12p40
pg/mL
C
IL-10
Mgl-1
IL-4
D
CHOP
GRP78
PDI
EDEM
E
CHOP
30 KDa
β–actin
42 KDa
Protein level (A.U.)
F
Protein carbonyl content (A.U.)
G
MitoSOX Red
Fluorescence per cell (A.U)